Determining the geochemical fingerprint of the lead fallout from the Notre-Dame de Paris fire: Lessons for a better discrimination of chemical signatures

Justine Briard, Sophie Ayrault, Matthieu Roy-Barman, Louise Bordier, Maxime L'Héritier, Aurélia Azéma, Delphine Syvilay, Sandrine Baron

Determining the geochemical fingerprint of the lead fallout from the Notre-Dame de Paris fire: lessons for a better discrimination of chemical signatures

Justine Briard [1], Sophie Ayrault [1,*], Matthieu Roy-Barman [1,†], Louise Bordier [1], Maxime L'Héritier [2], Aurélia Azéma [3], Delphine Syvilay [3], Sandrine Baron [4]

[1] Laboratoire des Sciences du Climat et de l'Environnement, LSCE UMR 8212, CEA – CNRS - UVSQ, Université Paris Saclay, France

[2] Archéologie et Sciences de l'Antiquité, ArScAn UMR 7041, CNRS, Université Paris 8, France

[3] Laboratoire de Recherche des Monuments Historiques, CRC USR 3224, Muséum National d'Histoire Naturelle - CNRS - Ministère de la Culture, France

[4] Laboratoire Travaux et Recherches Archéologiques sur les Cultures, les Espaces et les Sociétés, TRACES UMR 5608, CNRS - Université de Toulouse, France.

* Corresponding author: Sophie AYRAULT. Address: Laboratoire des Sciences du Climat et de l'Environnement (LSCE), bât 714, Orme des Merisiers, CEA Saclay, 91191 Gif-sur-Yvette, France

Phone + 33 1 69 08 40 71; **Email:** sophie.ayrault@lsce.ipsl.fr

ORCID: 0000-0001-8320-6917 (S.A.); 0000-0002-3986-4549 (M. R.-B.); 0000-0003-3428-2977 (M L'H.); 0000-0003-1910-8903 (S.B.)

† Deceased author

Determining the geochemical fingerprint of the lead fallout from the Notre-Dame de Paris fire: lessons for a better discrimination of chemical signatures

Abstract: (300 words max)

On 2019, the fire of Notre-Dame de Paris cathedral ("NDdP") spread an unknown amount of lead (Pb) dust from the roof of the cathedral over Paris. No data describing the geochemical fingerprint of the roof lead, as well as no particle collected during the fire, were available: a post-hoc sampling was performed. To discriminate the potential environmental impact of the fire from multiple Pb sources in Paris, it was mandatory to define unequivocally the fire dust geochemical signature. A dedicated and in hindsight geochemistry-based strategy was developed to eliminate any source of potential contamination due to sampling substrates or previously deposited dust. Radiogenic Pb isotopic signatures ($^{206}Pb/^{207}Pb$ and $^{208}Pb/^{206}Pb$ ratios) and elemental ratios were determined in 23 Pb-rich samples collected inside NDdP. We determined that the dust collected on wood substrates on the first floor was most representative of fire emissions. These samples were the analyzed for the 4 Pb isotopes (204, 206, 207, 208) and the fire dust signature is characterized by ratio values of $^{206}Pb/^{207}Pb$: 1.1669 - 1.1685, $^{208}Pb/^{206}Pb$: 2.0981-2.1095, $^{208}Pb/^{204}Pb$: 38.307 – 38.342, $^{207}Pb/^{204}Pb$: 15.633 – 15.639 and $^{206}Pb/^{204}Pb$: 18.242 – 18.275. In addition, the fire dust presents typical element-to-Pb ratio. This fingerprint was compared to the signatures of the known local Pb sources. The geochemical fingerprint of the fire is significantly different from that of the dominant urban Pb source. This will allow future evaluation of the contribution of the fire to Paris Pb pollution and of the real extent of the area affected by the Pb-containing dust plume. Moreover, the geographical origin of Pb used to for the roof restauration and the spire

47 building was identified. These findings open new ways to study the Pb sources in historical
48 monuments for environmental impacts evaluation, as well as for historical perspectives.

49 **Keywords:** historical monuments; lead isotopes; metals; environmental pollution; tracing
50 pollution

51

52

1. Introduction

Limiting lead pollution in an urban context is a major societal issue because this neurotoxic metal has significant consequences on health, especially for children (e.g., Laidlaw and Taylor, 2011; Landrigan et al., 2017). Notre-Dame de Paris cathedral (hereafter noted "NDdP"), an emblematic monument of the Gothic architecture, is an iconic French monument. The fire that took place on April 15, 2019, destroyed a large part of its lead-made roof and spire. During the following days, citizens and the scientific community took great interest in lead (Pb) pollution in the Parisian environment (Smith et al., 2020; van Geen et al., 2020; Vallée et al., 2021). A tentative estimation suggests that 150 kg of Pb was spread during the fire (Tognet and Truchot, 2019). Another study, based on the analysis of various soil samples, estimated that the fire plume deposited one ton of Pb within 1 km of the cathedral, suggesting that most of the fallouts occurred at a short distance of the cathedral (van Geen et al., 2020). A study was performed, involving adults living or working in the nearby of the cathedral, to highlight a variation in blood Pb levels (BLL). No increase in BLL was observed (Vallée et al., 2021), tending to show that the fire emission did not affect the Parisian population. The reality of an environmental impact of the fire is less clear. The analysis of dusts and soils collected in tree pits, parks and streets surrounding NDdP tends to show higher Pb concentrations for the samples collected under the plume (van Geen et al., 2020). Nevertheless, high Pb concentrations around NDdP after the fire do not necessarily mean that the fire is now the main source of Pb to Parisian soil. Indeed, a considerable spatial heterogeneity of the urban contamination results from the mixture of sources changing over time and space and from accumulation and erosion mechanisms (van Geen et al., 2020).

Lead contamination in Paris is an old story as seen in other major cities even though the drivers of contamination (past use of Pb additives in gasoline, deterioration of exterior paint, industrial emission, water supply) may differ from one city to another depending on its historical development (Delile et al., 2016, Laidlaw et al. 2017; Delile et al, 2017). The ban of leaded gasoline and other lead-containing products (e.g., lead paints) has drastically reduced the concentration of Pb worldwide (e.g., Shotyk et al., 2005; Marx et al., 2016). However, pervasive contamination is still observed in urban environments, such as Paris (France) and London (UK) cities, where many sources of Pb still exist (e.g., roofs, paintings, waste incinerators) (Ayrault et al., 2012, 2014; Resongles et al., 2021). To evaluate the potential impacts of the NDdP fire, it is therefore essential to accurately define the geochemical fingerprint of the fire by its Pb isotopic signature (Cheng and Hu, 2010; Ayrault et al., 2012; Rosca et al., 2018) and by its elemental signature (Font et al., 2015; Lin et al., 2015). Such an extended fingerprint is required in the context of urban environments where the Pb concentration alone cannot demonstrate the environmental impact of leaded roofs, an approach that proved valuable only in rural contexts where no other Pb source is observed (Jørgensen and Willems, 1987).

Consequently, the use of Pb isotope ratios is mandatory to identify the origin of the high Pb concentrations. Indeed honey samples were collected in Paris in the months following the fire and their composition (Pb isotopes and elements) was analyzed (Smith et al., 2020). Even though the median Pb isotope ratio of the honey samples (median $^{206}Pb/^{207}Pb$ ratio of 1.157±0.003) similar to the signature of the Pb urban background of Paris ($^{206}Pb/^{207}Pb$ ratio of 1.157±0.003, Ayrault et al., 2014), the Pb content of the honey collected under the plume trajectory was attributed to the NDdP fire (Smith et al., 2020). Such a conclusion cannot be

drawn without a comparison of the environmental samples with the fire emission signature. Unfortunately, no atmospheric particle was sampled during the fire.

Glorennec et al. (2021) determined the Pb isotope ratio in dust collected during July 2020 with wet wipes on different substrates inside NDdP (n=8) and roof remains (n=8). The sampling method used did not allow any elemental analysis or observations of the collected material, which could better constrain the fire emission signature or eliminate the risk of contamination of the samples with pre-fire dust. The determined fire isotopic signature ($^{206}Pb/^{207}Pb$: 1.167 ± 0.005) was considered ambiguous, preventing any evaluation of the potential impact of the fire due to the overlapping signature of other Parisian Pb sources. Nevertheless, we notice that this signature is different from today's urban Pb signature, which is distinctly low due to the imprint of leaded gasoline used during the second half of the 20th century.

To strip away the ambiguity about the environmental of NDdP fire, we performed a complete geochemical study (elemental and Pb isotope signatures (^{204}Pb, ^{206}Pb, ^{207}Pb, ^{208}Pb)) using all the available dust samples collected inside the cathedral. First, (1) we developed an appropriate step-by-step strategy to reveal the samples most representative of the fire emission. In addition, we proposed a robust protocol for future dust sampling in historical monuments. The objective is to be able to compare the data in the future (between monuments, after restoration works, and in case of another tragedy). (2) After selecting the samples representative of the dust emitted during the fire, we determined the geochemical signature of the leaded particles emitted by the fire. We compared the NDdP fire fingerprint with the different Pb sources already identified in the Parisian environment, to help with future environmental evaluation. (3) The geographical origin of the Pb ores used during the

restauration of the burnt roof and the construction of the spire was established. It is of interest for historical studies of Pb circulation during the 19th century.

A large range of elements were analyzed on the diverse samples collected in NDdP: the elements commonly analyzed in an urban context, such as Cd, Cu, Sb, and Pb (Le Gall et al., 2018; Smith et al., 2019), as well as elements, such as Ag, Sn and Bi, which can be associated with Pb in historical monuments (Sylvilay et al., 2015; L'Héritier et al., 2016; Comite et al., 2019). In addition, to document the signature of Pb used during the first stages of NDdP building, the Pb stable isotope ratio was also measured on "construction" Pb samples from Sainte-Chapelle and Chartres Cathedral, monuments contemporaneous to NDdP whose roofs have already burnt down (Shelby, 1981; Cohen, 2008).

2. Historical context

NDdP, located on the "Ile de la Cité" in the 4th arrondissement of Paris, is an emblematic monument in France (Figure 1A and 1B). Its construction was initiated in the second half of the 12th century by Maurice de Sully, who designed an exceptional monument that was 127 m long, 40 m wide and 33 m high (Figure 1C) and was the largest Christian monument at that time.

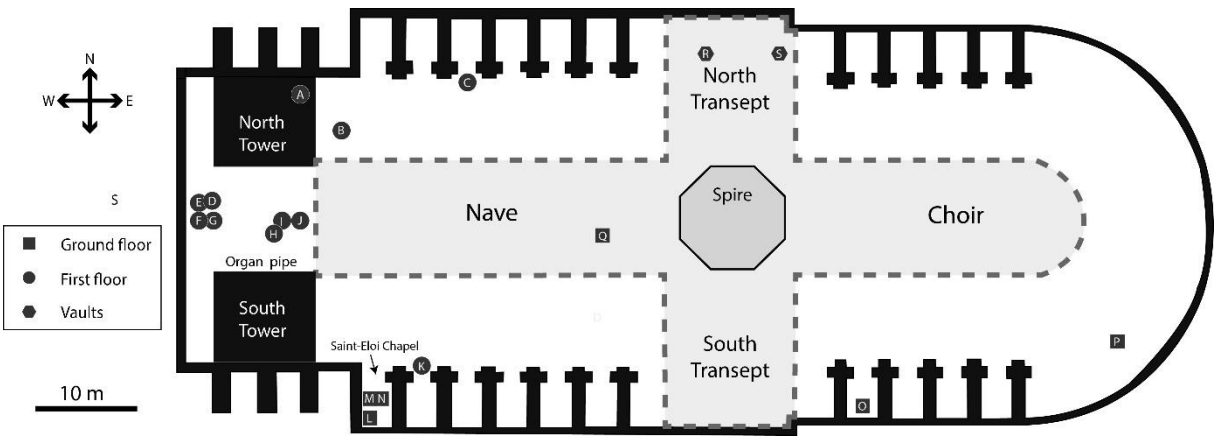

Figure. 1. Geographic context of Notre-Dame de Paris. A. Picture and B. location of this monument in Paris city. C. Map of Notre-Dame de Paris cathedral (modified after Aubert, 1920) and location of samples collected in this study (illustrated by the letters).

At the time of this study, NDdP was not yet accessible for sampling Pb joints, which are usually implemented in medieval construction to bind stones or seal iron armatures in early NDdP construction campaigns. Two major monuments coeval with original phases of construction of NDdP (late 12th-mid. 13th centuries) and located in the same region were chosen to determine the extent of the medieval Pb isotopic signature: Chartres cathedral (beg. 13th century) and the Sainte-Chapelle of Paris (mid. 13th century).

3. Materials and Methods

3.1 Fire dust and lead metal sampling

No NDdP sample was collected directly in the smoke plume or around the cathedral during or just after the fire. Indeed, intensive washing of the forecourt and roadway was conducted over the following days. In addition, access into the cathedral for scientists for dust sampling was denied until June 2019, where access was extremely limited. The fire dust deposited in the cathedral appeared to be the most appropriate material to represent the Pb particles likely to contaminate the environment, rather than sampling metallic remains of the burnt roof, which can exhibit different geochemical signatures depending on their construction and restoration phases (L'Héritier et al., 2016; Glorennec et al., 2021). Ideally, the dust samples should have been collected immediately after the fire and only on dedicated supports previously tested for their low element content. In practice, dust samples were collected whenever and wherever it was possible from June 2019 to February 2020 on several substrates (wood, metal, glass, fabric – described in Table S1) at the ground and first floors (Fig. 1). Dust from the vaults falling on the ground with the spire collapse was also collected.

Dust was collected with a polypropylene spatula, and the material was stored in a tightly closed polyethylene box. To clarify the comparison with previously published data, Glorennec et al. (2021) further sampled dust by using wet wipes at 8 of the 16 sites in the present study.

Subsequent binocular magnifying glass observations of the collected dusts highlight the presence of a “fiber and dust” fraction in 4 samples in addition to the “only dust” fraction present in all samples, e.g., the ND160919-01 sample collected on the stained-glass window revealed dust trapped in a fiber aggregate (Table S1). The two different matrices were analyzed separately. The “fiber and dust” fraction is collected from the original sample box with a plastic clamp; the latter is gently shaken to remove as much dust as possible from the fibers, and then the fibrous aggregate is placed in another plastic box. In addition, a paint fragment was identified and isolated in the dust of sample ND160919-01 collected on the stained glass window during microscopic observation. Two crusts of melted Pb were sampled using a chisel at 2 sites of the vaults (Table S1). To summarize, 23 samples are analyzed in this study: 16 “dust” samples, 4 “fiber and dust” subsamples, 2 “crust” samples and 1 “painting” fragment sample.

Metallic Pb samples of less than 1 cm in size were cut with a chisel on Pb joints directly in the studied buildings: Chartres cathedral (n=14) and the Sainte-Chapelle of Paris (n=8). These Pb samples were first analyzed by LA-ICP–MS to determine their element concentrations (L’Héritier et al., 2016). Then, Pb samples with low Sn contents (< 10 mg kg^{-1}), which are unlikely to come from recycling (Wyttenbach et al., 1973), were selected for Pb isotopic analysis.

3.2. Sample preparation

A total digestion procedure was applied (Le Gall et al., 2018). Samples (~1 to 12 mg) were introduced into closed PTFE beakers heated on a hot block (Digiprep, SCP Science) with ultra-pure concentrated acids (67% HNO_3: Normatom grade, VWR; 34-37% HCl, 47-51% HF, 65-71% $HClO_4$: TraceMetal grade, Fisher Scientific). The first step consisted of adding 4 mL HF and 2 mL $HClO_4$ for 6 hours at 150 °C, followed by evaporation to dryness. Second, aqua regia (5 mL) was added to the beakers heated at 120 °C for 3 hours. One mL of HNO_3 was added to the solution which was evaporated near dryness (3 times) before it was made up to 50 mL in HNO_3 0.5 N. The accuracy of the measured concentrations was checked using two certified reference materials (CRM: IAEA lake sediment SL-1 and IRMM road dust BCR-723) and a chemical blank.

Construction Pb samples were first scoured with a scalpel blade to remove the encrustation. A second scalpel blade was used to take 20 to 50 mg of pure Pb. These Pb pieces were cleaned 3 times with 1 mL of 5 N HNO_3 for 10 min. The cleaned pieces were then partly dissolved in 1 mL of 5 N HNO_3 for 10 min, and the solution was collected using a pipette.

3.3. Elemental composition analysis

Element concentrations were determined using a Thermo Scientific™ iCAP™ TQ ICP–MS equipped with a Peltier cooled cyclonic spray chamber, glass concentric nebulizer (400 µL min^{-1}) and 2.5 mm internal diameter quartz torch in Laboratory LSCE (Gif-Sur-Yvette, France). Two different measurement modes were selected in this study depending on the analyte analyzed and its interferants (Table S2). The certified riverine water standard SRM-1640a (National Institute for Standard Technology, NIST, USA) is additionally used to judge the calibration curve essential to propose concentration values. The concentration values obtained for the CRMs were within 15% of the certified values, and within 10% (except Mg

and Al: 30 %) for BCR-723 and SL-1, respectively. The standard deviation (SD) was lower than 5% except for Ag (10 %). For more details, see the Supporting Information.

3.4. Lead isotope composition analysis

LSCE: Pb isotope ratios ($^{208}Pb/^{206}Pb$ and $^{206}Pb/^{207}Pb$) were analyzed in the solutions that were also used for Pb concentration determinations. Analyses were also made with a Thermo Scientific™ iCAP™ TQ ICP–MS in Laboratory LSCE (Gif-Sur-Yvette, France). Mass bias and drift of the isotope ratios were corrected based on repeated measurements of the Pb reference material NIST SRM-981 that were analyzed between every two samples. The certified values used for the SRM-981 calculation are $^{206}Pb/^{207}Pb = 1.0933 \pm 0.0004$ and $^{208}Pb/^{206}Pb = 2.1681 \pm 0.0008$. The 2σ errors (2SD) of isotope ratios are 0.29% and 0.27% for the $^{206}Pb/^{207}Pb$ and $^{208}Pb/^{206}Pb$ ratios, respectively. The digestion blank was lower than 0.2 ng mL^{-1}, while the analyzed solutions were at 2 ng mL^{-1} after 100-100000 times dilution of the digestion solution. The $^{206}Pb/^{207}Pb$ and $^{208}Pb/^{206}Pb$ ratio measured for the CRM agree with the published values: 0.13% and 0.09%, 0.16% and 0.16%, for IAEA lake sediment SL-1 and IRMM road dust BCR-723, respectively (Table S3).

SARM: Among the whole samples batch, 11 were chosen to measure all the Pb isotopic ratios. These aliquots - which contain ~ 4 ng of Pb each - were sent to the SARM laboratory, a National Service of CNRS (https://sarm.cnrs.fr). After evaporation, each residue was taken back in bromidic acid (HBr) solution and loaded on anionic resin (AG1X8) to separate Pb from sample matrix (Manhes et al., 1980). Samples were analysed by using an MC-ICP-MS equipment (Neptune+ from Thermo). The NIST SRM 981 and NIST 997 Tl reference materials (ratio 1/10) were used to correct the instrumental mass bias (White et al., 2000). Values used for both reference materials were taken from Thirlwall (2002). The total procedural blank is

negligible in the entire session. The NIST-SRM 981 Pb precision and accuracy of all the reported isotopic ratios are better than 250 ppm (2SD). The $^{208}Pb/^{206}Pb$ and $^{206}Pb/^{207}Pb$ ratio results obtained at LSCE and SARM are in good agreement (supplement information, Fig S1.1).

4. Results

4.1. Elemental composition of NDdP samples

The Pb concentrations of the NDdP samples ranged from 24.6 to 967.9 g kg^{-1} (median: 160 g kg^{-1}; S3; Figure 2). The concentrations of the samples collected on wood, fabric, stained glass, metal substrates and the painting fragment were very close to the median value compared to the samples collected on crusts and in the vault dusts, where the Pb concentrations were 3 times higher.

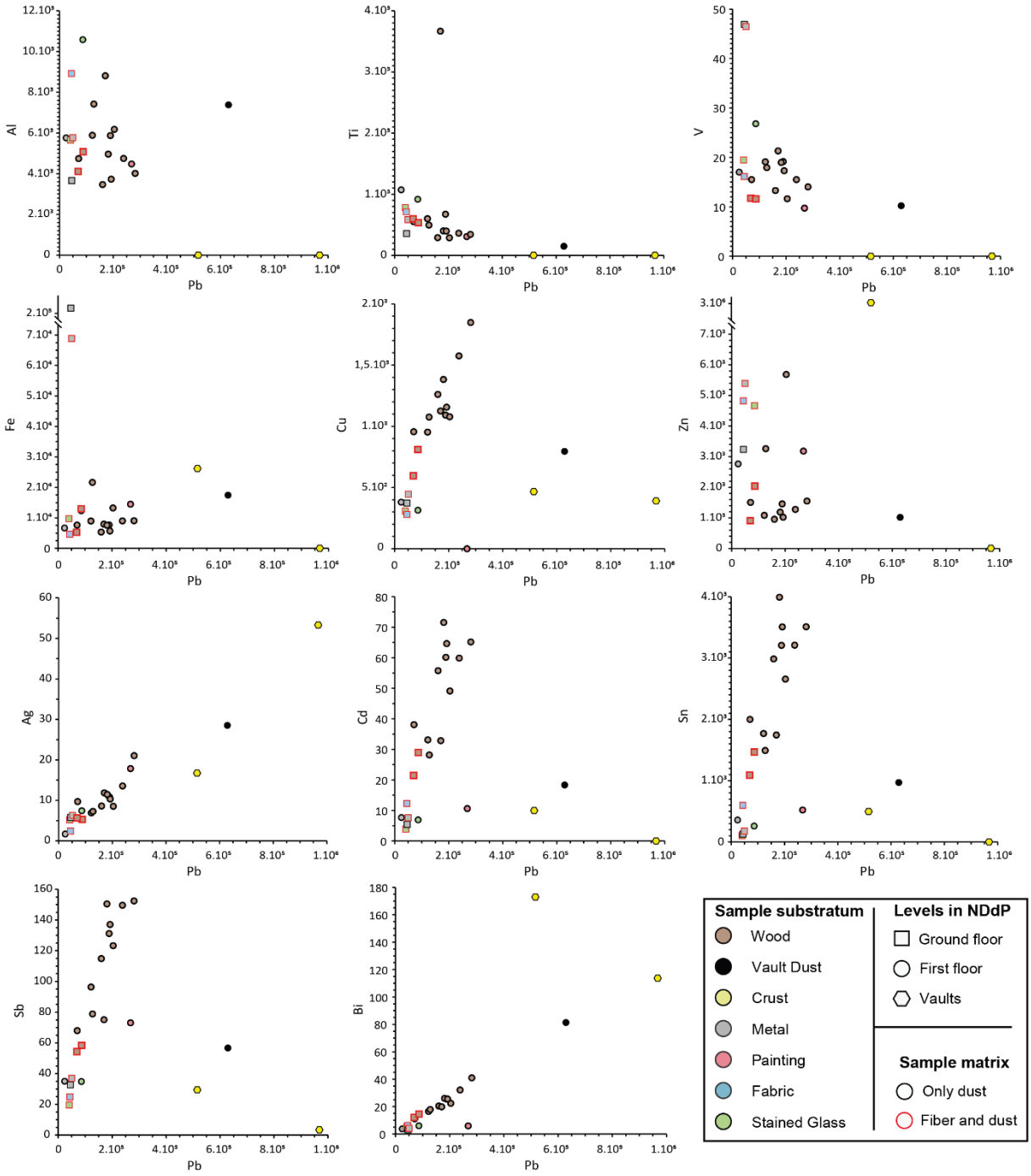

Fig. 2. Bivariate concentration plots of selected element concentrations versus Pb concentrations for NDdP samples collected from 2019–2020 by the LRMH laboratory (unit: mg kg^{-1}). Each color corresponds to a substrate type where the dust samples were collected (brown = wood; black = vault dusts; yellow = crust; gray = metal; pink = painting; blue = fabric; green = stained glass) and the symbol corresponding to the level of collected substrate in NDdP (square = Ground floor; circle = First floor; hexagon = Vaults). The sample matrix is represented by the outline color of the dots; the black outlines correspond to the dust-only fraction, and the red outlines correspond to the fiber and dust fraction.

For the other elements, the concentration depended on the substrate (Figure 2). This was particularly the case for Fe and V, where the most concentrated samples were collected on the metal substrate. The samples with the highest concentrations in Cu, Cd, Sn and Sb,

were collected on wood substrate. The samples collected on crusts and vault dusts were enriched in Ag and Bi. Moreover, Ti and Zn concentrations were very variable, with a single sample collected on wood rich in titanium and a single sample collected on a crust rich in zinc. Al concentrations are generally higher, especially for the dusts collected on the fabric and on the stained glass and with the exception of the two crust samples. Concentrations of the other measured elements are given in Table S4.

4.2. NDdP samples and other historical monuments lead isotope compositions

Each sample analyzed for elements was also measured for radiogenic Pb isotopes to determine the $^{208}Pb/^{206}Pb$ and $^{206}Pb/^{207}Pb$ ratios at LSCE (Figure 3). The $^{206}Pb/^{207}Pb$ values range between 1.1584 ± 0.0040 and 1.1780 ± 0.0033 (median: 1.1684) and $^{208}Pb/^{206}Pb$ values ranging between 2.0896 ± 0.0057 and 2.1051 ± 0.0113 (median: 2.0971). The isotopic results highlighted two endmembers depending on the substrate. The first isotopic endmember characterized by a high $^{208}Pb/^{206}Pb$ ratio and a low $^{206}Pb/^{207}Pb$ ratio was represented by the samples collected on the outdoor crusts and a sample collected on the wood substrate, while the second isotopic endmember characterized by a low $^{208}Pb/^{206}Pb$ ratio and a high $^{206}Pb/^{207}Pb$ ratio was represented by the painting fragment and the samples collected on the stained glass window and metal substrate (Figure 3; Table S4). The Pb isotope ratios of samples collected

on wood, fabric and vault dusts vary between these two endmembers.

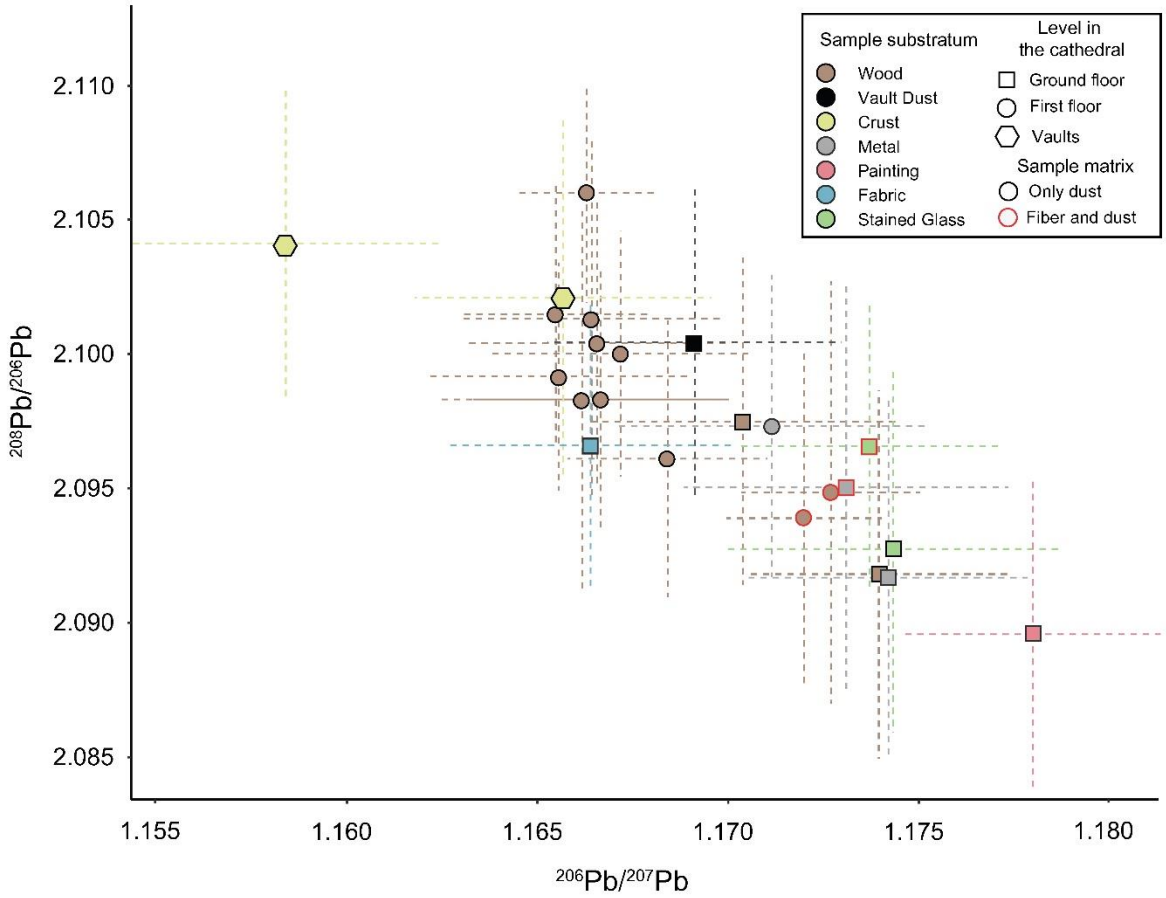

Fig. 3. Lead isotopic compositions of all NDdP samples from this study. The symbol corresponds to the level of collected substrate in NDdP (square = ground floor; circle = first floor; hexagon = vaults), and the color corresponds to substrate type where samples were collected in cathedral (brown = wood; black = vault dusts; yellow = crust; gray = metal; pink = painting; blue = fabric; green = stained glass). The sample matrix is represented by the outline color of the dots; the black outlines correspond only to the dust fraction, and the red outlines correspond to the fiber and dust fraction.

The samples representative for the NDdP fire dust (n=9, see section 5.1) were also measured for Pb isotopes to determine the ratios $^{208}Pb/^{204}Pb$, $^{207}Pb/^{204}Pb$ and $^{206}Pb/^{240}Pb$ ratios at SARM. The Pb isotopic signatures average (median values) 18.252 ± 0.001 for $^{206}Pb/^{204}Pb$, 15.634 ± 0.002 for $^{207}Pb/^{204}Pb$ and 38.307 ± 0.007 for $^{208}Pb/^{204}Pb$ (Table S7).

4.3. Lead isotope compositions of lead artifacts from other historical monuments

The Pb isotopic signatures obtained in construction Pb of the Sainte-Chapelle ranged between 1.1760 ± 0.0089 and 1.1856 ± 0.0138 (median: 1.1829) for $^{206}Pb/^{207}Pb$ values and between 2.0736 ± 0.0086 and 2.1011 ± 0.0259 (median: 2.0828) for $^{208}Pb/^{206}Pb$ values. They are generally consistent with the Chartres cathedral results, with values ranging between 1.1793 ± 0.0065 and 1.1882 ± 0.0103 (median: 1.1858) for $^{206}Pb/^{207}Pb$ ratios and between 2.0616 ± 0.0202 and 2.0914 ± 0.0139 (median: 2.0771) for $^{208}Pb/^{206}Pb$ ratios (Table S5).

5. Discussion

5.1. Defining the dust samples representative of the NDdP fire emissions

Knowing that no dust sample could be directly sampled in the plume, our first purpose is thus to select samples representative of the dust emitted during the fire and to propose a sampling scheme that could be applied to historical monuments.

The first step of the procedure is the binocular observations, which allowed to separate the mixture of fibers and dust for 4 samples revealed primarily a homogeneity of the Pb isotope ratios (Figure S1) unrelated to the substrate but lower elemental concentrations compared to the “only dust” fraction (Figure S2; Table S6), which may suggest dilution and/or contamination of the NDdP fire signature by the presence of fibers. The elemental content and the Pb isotope ratio obtained for the “only dust” fraction with respect to the data obtained in the “fiber and dust” fraction are discussed in depth in the Supporting Information. Following this discussion, we will focus on the “only dust” more representative of the NDdP fire for the remainder of this discussion.

The second step relies on the elemental analysis data, to infer any contamination from the sampling substrate (Fig. 2). The observed large concentration scattering can be linked to

303 a potential contamination originating from the substrate. Such contamination is well known,
304 and for atmospheric particle collection, inert (plastic) substrates are recommended (Amodio
305 et al., 2014). This is potentially the case for crust samples. SampleND140619-01 was collected
306 on ridge crest reinforcements and could only represent the local melted Pb. ND140619-04 was
307 collected on an outdoor upper surface stone where current urban pollution is plausible. Thus,
308 These two samples were no more considered.

309 The vault dust (ND080719-02) collected indoor on the pavement of NDdP could be a
310 mixture of the fire emissions with rubble and other various debris coming from the structure
311 of NDdP roof. The elemental composition of the painting fragment isolated in the dust of
312 sample ND160919-01 testifies to a local signature characteristic of one paint used during one
313 of the numerous renovation episodes of NDdP and cannot represent the fire signature.

314 Elemental concentrations lower than the average of content were found for 3 dust
315 samples: sample ND160919-04 collected on iron armatures, sample ND160919-01 collected
316 on stained glass and sample ND140619-07 collected fabrics (Fig. 2). The first one presents
317 high Fe concentration while the two later present high Al content (Fig. 2). These high Fe and
318 Al concentrations may evidence contamination by the substrate, implying a less obvious
319 contamination for other elements. Moreover, several Pb sources can originate from the
320 stained glass windows: anti-rust paints of the iron armatures, Pb joints of the window
321 masonry and Pb cames. Thus, these three samples were discarded.

322 To approach the fire signature, it is essential to focus on an inert substrate. Figure 2
323 shows that the samples collected on wood show very consistent elemental content. Wood is
324 naturally poor in metals, except in areas with high metal contamination (Watmough and
325 Hutchinson, 1996; Yu et al., 2007; Sawidis et al., 2011). Previous studies exhibited

concentrations ranging from 0.1 – 5, 5 – 10, 0.5 – 30 and 1 – 20 mg kg^{-1} for Pb, Zn, Cu and Ni, respectively, in Scots pine and Norway spruce wood (Harju et al, 1996; Saarela et al., 2005). These values are far lower than the concentrations in NDdP dust. Thus, the potential contamination of the samples by the wood substrate is considered negligible. By estimating that the elemental signature of the NDdP fire corresponds only to the dust fraction of the 9 samples collected on wood furniture, the Pb concentration range was between 70.9 and 281.6 g kg^{-1} (median: 181 g kg^{-1}), which is the most concentrated element (Fig. 2; Table S4).

To refine the choice of the samples most representative of the fire emission, we combined the elemental ratios with the Pb isotopic ratios. To understand the isotopic variability of the dust collected on the wood substrate (Fig. 3), we questioned the impact of the dust location in the building; namely the ground floor, the first floor or the vault. We observed that the height of the sample in the cathedral affects the Pb isotopic signature: high isotopic values in $^{206}Pb/^{207}Pb$ for dust sampled at ground level and low isotopic values in $^{206}Pb/^{207}Pb$ for samples collected at the first floor (Fig. 3). A potential contamination by preexisting accumulated dust can explain this difference between the samples of the first floor and the ground floor. Indeed, while it is complex to estimate the cleaning frequency of all the substrates, the wood-made furniture (such as the altar or the seats) are frequently dusted. This is particularly true for the organist bench (ND140619-06) which is known to be frequently cleaned and the organist was notably performing on the evening of the fire. Furthermore, this isotopic difference could also have been produced by a heterogeneous air flow and dust deposition between upper (first floor) and lower parts (ground floor) during the fire. In particular, the spire fall could have caused the fall of coarser dust (i.e., stone and wood debris) on the lower parts. As a consequence, the dust collected on the cathedral ground floor was not composed only of fire dust. Indeed, with the exception of Zn and Al, the samples from the

ground floor seem to have lower Cu, Cd, Sn, Sb, Pb and Bi concentrations than the samples collected on the first floor, although the difference is subtler (Figure 2). These lower element concentrations can be explained by a considerable dilution by the important quantity of coal and rubble in the dust collected at the ground floor. Consistently with the elemental data, the dust collected on the wood substrate of the first floor shows very congruent Pb isotopic measurements.

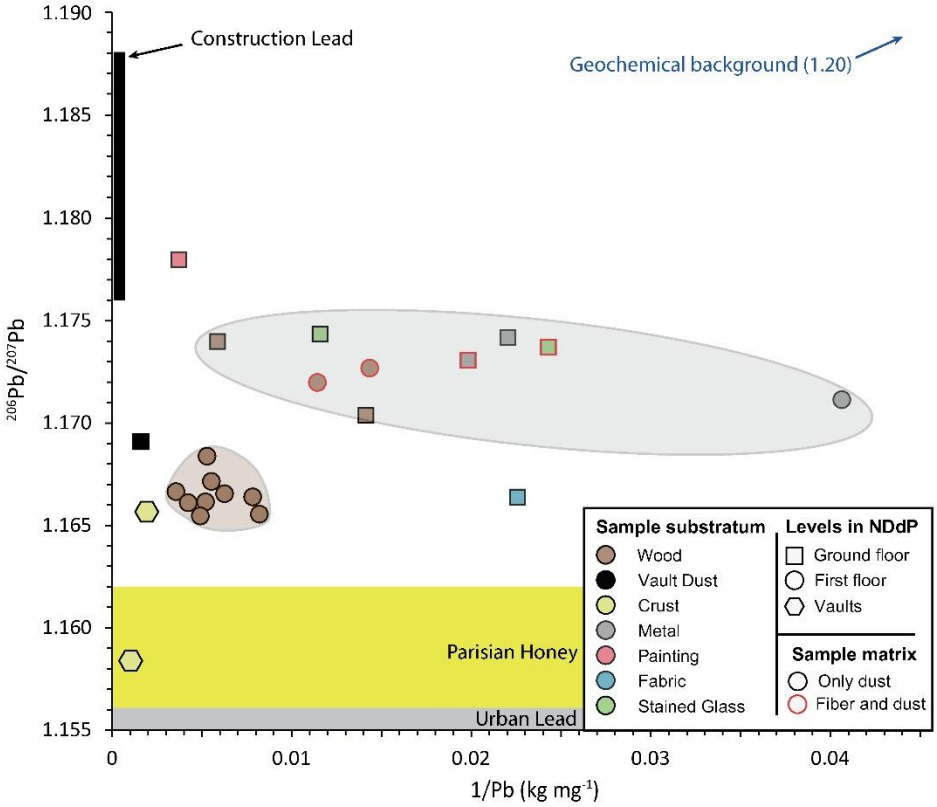

Fig. 4. $^{206}Pb/^{207}Pb$ ratio of all analyzed NDdP dusts as a function of the 1/[Pb] ratio (kg mg^{-1}). The symbol corresponds to the level of collected substrate in NDdP (square = ground floor; circle = first floor; hexagon = vaults), and the color corresponds to substrate type where samples were collected in cathedral (brown = wood; black = vault dusts; yellow = crust; gray = metal; pink = painting; blue = fabric; green = stained glass). The sample matrix is represented by the outline color of the dots; the black outlines correspond only to the dust fraction, and the red outlines correspond to the fiber and dust fraction.

We conclude that the fire signature can be better approached by the dust collected on the wood substrate of the first floor. Figure 4 shows that these samples (brown circles) design a clearly defined and sharp area with converging Pb isotope ratio and high Pb content. This

area is very distinct from the one grouping the other samples collected in NDdP. Those samples, while having a very scattered Pb content, have quite homogeneous Pb isotope ratio which could be interpreted as the signature of the Pb present in the NDdP indoor dust before the fire. The validation of this hypothesis would need a dedicated work, which may rely on a comprehensive comparison of the geochemical signature of dust collected in coeval unburnt monuments such The Sainte Chapelle (Paris).

5.2. Identifying and tracing the leaded NDdP fire emissions in the Parisian environment

The most appropriate samples (i.e., collected on wood substrate at the first floor) defined the signature of the NDdP fire with values in $^{206}Pb/^{207}Pb$ between 1.1655 ± 0.0025 and 1.1684 ± 0.0043) and values in $^{208}Pb/^{206}Pb$ between 2.0961 ± 0.0042 and 2.0961 ± 0.0113 with median values at 1.1664 ± 0.0034 and 2.1000 ± 0.0051 respectively. These ratio values are consistent with those proposed by Glorennec et al. (2021) for dust samples $^{206}Pb/^{207}Pb$ ratio: 1.167 ± 0.005. Among the 8 dust samples collected by Glorennec et al (2021), 4 are out of the area defining the NDdP fire signature because of outliers in the determination of the ratio $^{208}Pb/^{206}Pb$ (Fig. 5). The here determined signature of ~~the~~ NDdP fire is more accurate, opening the way to a reliable evaluation of its uniqueness among the other sources of Pb in the Parisian environment.

During the 20th century, three Pb signatures were identified in Paris city (Ayrault et al., 2012): (1) Pb used during the 19th century for Haussmann's renovation of Paris city, imported from Spain (Lestel, 2012), imprinting the Seine River sediment before 1960 and after 2000 which $^{206}Pb/^{207}Pb$ ratio is ≈ 1.1650 ± 0.0025 and $^{208}Pb/^{206}Pb$ ratio is ≈ 2.1047 ± 0.0046 (Ayrault et al., 2012); (2) Pb used in leaded gasoline ($^{206}Pb/^{207}Pb$ =1.08 ± 0.02 and $^{208}Pb/^{206}Pb$ ratio is ≈ 2.18 ± 0.02 (Monna et al., 1997; Véron et al., 1999)), used until its ban on 2000, containing

high proportions of Australian Pb from the Broken Hill mine; and (3) the local natural background signature ($^{206}Pb/^{207}Pb$=1.201 ± 0.001, $^{208}Pb/^{206}Pb$=2.0527 ± 0.0020; (Elbaz-Poulichet et al., 1986)), which appears negligible in downtown Paris but can be detected in less urbanized areas. A fourth Pb source, the dominant Pb isotopic signature in Paris street dust, called the "urban" Pb, is characterized by relatively high $^{208}Pb/^{206}Pb$ ratios (range: 2.088–2.115; median: 2.107) and low $^{206}Pb/^{207}Pb$ ratios (range: 1.142–1.166; median: 1.155) (Figs 4 and 5) and represents a mixture of urban Pb and leaded gasoline (Ayrault et al., 2014). Indeed, the pervasive contamination of the urban environment due to banned leaded gasoline was also observed in London (Resongles et al., 2021).

Not surprisingly, the signature of ~~the~~ NDdP fire is far from the geochemical local background. The fire Pb signature of the burnt roof (XIXe) is logically different from the construction Pb signatures (Fig. 5). The age of historical monuments whose signatures are showed oscillates between the 12th and 13th centuries (e.g., Sainte-Chapelle in Paris and Chartres Cathedral; Table S5) and the 17th century (Versailles Palace; Pons-Branchu et al., 2015) with $^{206}Pb/^{207}Pb$ ratios ranging between 1.1760 ± 0.0089 (Sainte-Chapelle de Paris) and 1.1882 ± 0.0103 (Chartres Cathedral) (Table S5; Figure 5). Three of the 8 undated Pb artifacts collected by Glorennec et al. (2021) lie in this area drawn by the 12th – 17th construction Pbs.

Most importantly, the NDdP fire geochemical signature is significantly different from today's urban Pb signature (Fig. 5) represented by municipal solid waste combustors (Widory et al., 2004) and wastewater suspended particle matter (Ayrault et al, 2012). On the opposite, the "urban" signature is found on PM_{10} fine particles collected in Paris in 2003 (Widory et al., 2004) and in honey produced in Paris and collected within 6 months after the fire (Smith et al., 2020). Despite their high Pb content, it shows that the honey samples did not register the

NDdP fire emissions but the pervasive urban Pb. Indeed, soils and honeys are potentially likely to collect all the urban Pb sources present in Paris before, during and after the fire.

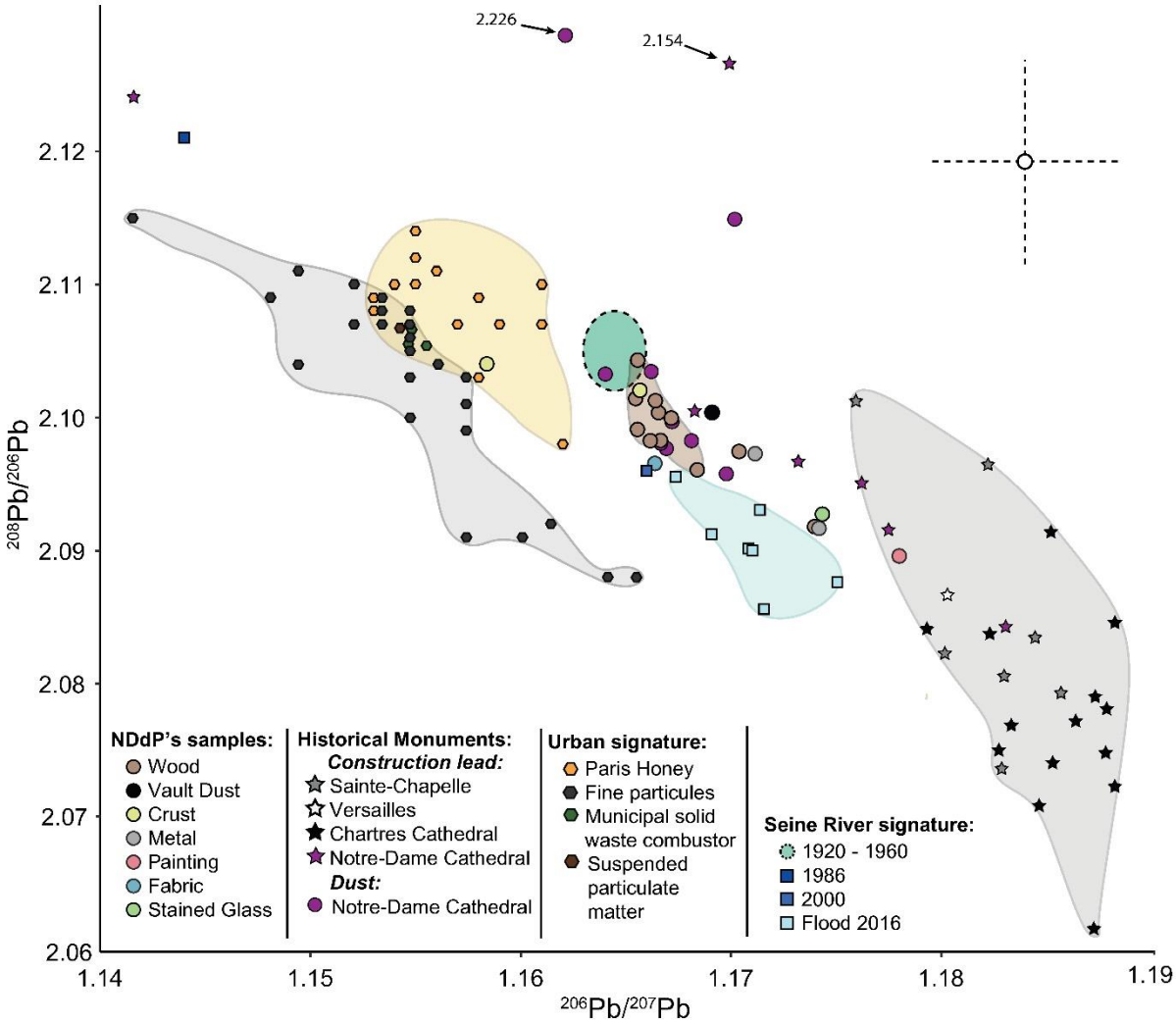

Fig. 5. Lead isotopic composition of all analyzed NDdP samples and historical monuments (Sainte-Chapelle and Chartres Cathedral) from this study compared with local anthropogenic sources, and other historical monuments. Dust and Pb artifacts from a previous study collected in NDdP are also shown (purple circles and stars, Glorennec et al., 2021). Other sources include Versailles Palace (Pons-Branchu et al., 2015), Paris honey (Smith et al., 2020), fine particles (Widory et al., 2004), municipal solid waste combustors (Widory et al., 2004), wastewater suspended particle matter (Ayrault et al, 2012)and separate Seine River signatures with ratios obtained between 1920-1960 in 1986 in 2000

(Ayrault et al., 2012) and the Seine River flood in 2016 (Le Gall et al., 2018). The typical errors of NDdP samples (this work) are lower than 0.0044 and 0.0078 in $^{206}Pb/^{207}Pb$ and $^{208}Pb/^{206}Pb$, respectively.

The NDdP fire Pb isotope signature is close to the isotopic signature of the Seine River sediments collected after 2000 (Ayrault et al., 2012). The Seine River Pb contamination results from the Pb used during the construction of the Hausmannian Paris, which is contemporaneous of the last large restauration of the NDdP roof. We hypothesize that the Pb used for ~~the~~ NDdP restauration and its spire construction was of the same origin as Pb used for the Hausmann buildings. Therefore, it will be fundamental to couple the elemental ratios and the Pb isotope ratio, and may be also carbon isotopes (Widory et al, 2004) to evaluate the impact of ~~the~~ NDdP fire on the Seine River sediment contamination.

The NDdP fire dust concentrations of Pb and some elements are clearly higher than those found in an urban context (Pio et al., 2013; Font et al., 2015; Smith et al., 2019; 2020). Some are companion elements of Pb (Cu, Ag, Sb, Bi). Consistently, the concentration of Pb and the concentrations of these elements are correlated (Table 1). Tin (Sn) presents also high concentrations in the NDdP fire dust. van Geen et al. (2020) also noted high Sn concentration in the soil samples collected at the proximity of the cathedral and suggested that the Sn/Pb ratio could be used as a fire marker. Unfortunately, no Sn-Pb correlation was found in the dust samples representative of the NDdP fire, preventing the use of Sn/Pb ratios as a fire marker. The origin of Sn in ~~the~~ NDdP fire dust can be the anti-corrosion coating applied on the Pb tables and/or the use of Sn in solder used for welding. These diverse uses of Sn may explain why Sn and Pb are not correlated.

The elemental ratios for the NDdP fire dust are compared to ratios observed in urban environmental atmospheric particle and street dust samples Table 1). In literature, several elemental ratios are used to trace the road traffic signature in urban environments. Indeed,

449 road traffic is an important source of inorganic contaminants to the Parisian environment
450 (Gasperi et al., 2021), and elemental ratios are powerful tools to examine the impact of traffic-
451 related metal and metalloid sources (e.g., Charlesworth et al., 2011). The Sb/Cu ratio, widely
452 used in tunnels (Lin et al., 2015), ranges between 0.08 and 0.88 with an average of 0.16 (Gillies
453 et al., 2001; Pio et al., 2013). The Sb/Cu ratio of NDdP is 0.10±0.02 (0.07 – 0.12), which is not
454 distinct enough from the road traffic signature to be use as a NDdP fire marker. Interestingly,
455 the NDdP Sb/Cu ratio appears to be higher than the Sb/Cu ratio of 0.021 determined from
456 elemental data from the Parisian honey study (Smith et al., 2020), confirming that the honey
457 collected within 6 months after the fire did not register the fire emissions. The Sn/Cu ratio can
458 also be used to trace the road traffic signature.

459 **Table 1. Elemental ratio calculated for the NDdP fire signature obtained for the 9 samples**
460 **representative of the NDdP fire (Pearson test < 0.05) and values proposed in the literature.**

	This study						
Ratio	Median	SD	Range	R^2	p value	Parisian honey (Smith et al., 2020)	Tunnel dust (Lin et al., 2015)
Cu/Pb	0.0066	0.001	0.0053 – 0.0084	0.71	0.004	5.16	-
Sb/Pb	0.00069	0.00009	0.00054 – 0.00083	0.70	0.005	0.114	-
Cd/Pb	0.00027	0.00006	0.00022 – 0.00039	0.47	0.042	0.011	-
Bi/Pb	0.00013	0.00001	0.00011 – 0.00015	0.92	< 0.0001	-	-
Ag/Pb	0.000057	0.000009	0.000042 – 0.000075	0.82	0.001	-	-
Sb/Cu	0.10		0.07 – 0.12	0.88	0.029	0.021	0.08-0.88

461

462 To conclude, these findings leave some space to use Pb isotopes as an indicator of the
463 presence or absence of NDdP fire Pb in Parisian environment (streets, playgrounds …), at least

in favorable cases (i.e., low pre-fire Pb contamination). Element (Cu, Sb, Ag, Bi) to Pb concentration ratio can be used as additional marker of the fire dust deposition extent.

5.3. Locating the ore origin(s) of the burnt roof.

To identify the geographic origin of the Pb of the Notre Dame fire dust, the $^{208}Pb/^{204}Pb$ versus $^{206}Pb/^{204}Pb$ ratio and $^{207}Pb/^{204}Pb$ versus $^{206}Pb/^{204}$ Pb ratio were performed (Table S7) to refine the characterization by the use of ^{204}Pb, which is stable since the Earth formation's. Ellam et al. (2010) demonstrated that several Pb sources are not distinguished if the ^{204}Pb isotope is not considered in the ratio. Indeed, $^{206}Pb/^{204}Pb$ ratios coupled with $^{208}Pb/^{204}Pb$ and $^{207}Pb/^{204}Pb$ ratios are commonly used in mining and chemical geology but also in archaeometry to determine the lead sources and the exchanges between the different countries over time (Baron et al., 2006; Bode et al., 2009).

Pb used during the 19th century - very large quantities of Pb were needed for Haussmann's renovation of Paris city and the restoration of NDdP and Sainte Chapelle's roofs - was largely imported in France from Spain (Lestel, 2012). The isotopic signatures obtained on the selected samples from NDdP were compared with those of Pb ores from southern Spain, the most active Pb mines, currently available in the literature.

The isotopic signatures of the ores plotted on the $^{208}Pb/^{204}Pb$ versus $^{206}Pb/^{204}Pb$ diagram (Figure 6) are very heterogeneous, especially for Cartagena mining district. The signatures of the Rio Tinto and La Carolina mining districts are relatively homogeneous, at this scale of study. The La Carolina isotopic signatures overlap one of the three isotopic composition fields of Los Pedroches and the Rio Tinto one. These signatures reflect the complex geological history of these large mining areas in southern Spain. Two different mixing lines are highlighted here. They reflect the signature of two different metallogenic sources. The first

one, which is the most radiogenic, is constituted by the isotopic signatures of a part of the ores from Cartagena. The second one, less radiogenic, is composed by the isotopic signatures of Rio Tinto, La Carolina, Los Pedroches and a part of Cartagena ores. This suggests a common origin of the mineralization fluids, which is different from the first one. The isotopic signatures of the NDdP fire dust are aligned with the second mixing line suggesting that its Pb is coming from Rio Tinto, La Carolina, Cartagena and partially from Los Pedroches ores.

Nevertheless, with respect to the $^{207}Pb/^{204}Pb$ versus $^{206}Pb/^{204}Pb$ ratios, different isotopic fields are highlighted within a same mining district which is the case for Los Pedroches and Cartagena. This suggests that the mineralization phase occurred in several episodes of mineralization (3 for Los Pedroches and 2 for Cartagena). In the case of Rio Tinto and La Carolina, the ores come from a single phase of mineralization emplacement and also have a common origin.

The isotopic signatures of the NDdP fire dusts are, again, aligned along a mixing line formed by the least radiogenic group of Cartagena ores. The other mining districts of Los Pedroches, La Carolina and Rio Tinto are excluded. One of the phases of Los Pedroches and those of La Carolina and Rio Tinto are almost synchronous. The NDdP fire dust therefore seem to have originated from Cartagena mining district.

In addition, the fire dust signature is more precise and comprehensive using the data obtained at SARM. Finally, the Pb isotope ratio of the leaded particles emitted by the 2019 fire are: $^{206}Pb/^{207}Pb$: 1.1669-1.1685, $^{208}Pb/^{206}Pb$: 2.0981-2.0995, $^{208}Pb/^{204}Pb$ ratios: 38.297 - 38.342, $^{207}Pb/^{204}Pb$: 15.633 - 15.639 and $^{206}Pb/^{204}Pb$: 18.242 – 18.275.

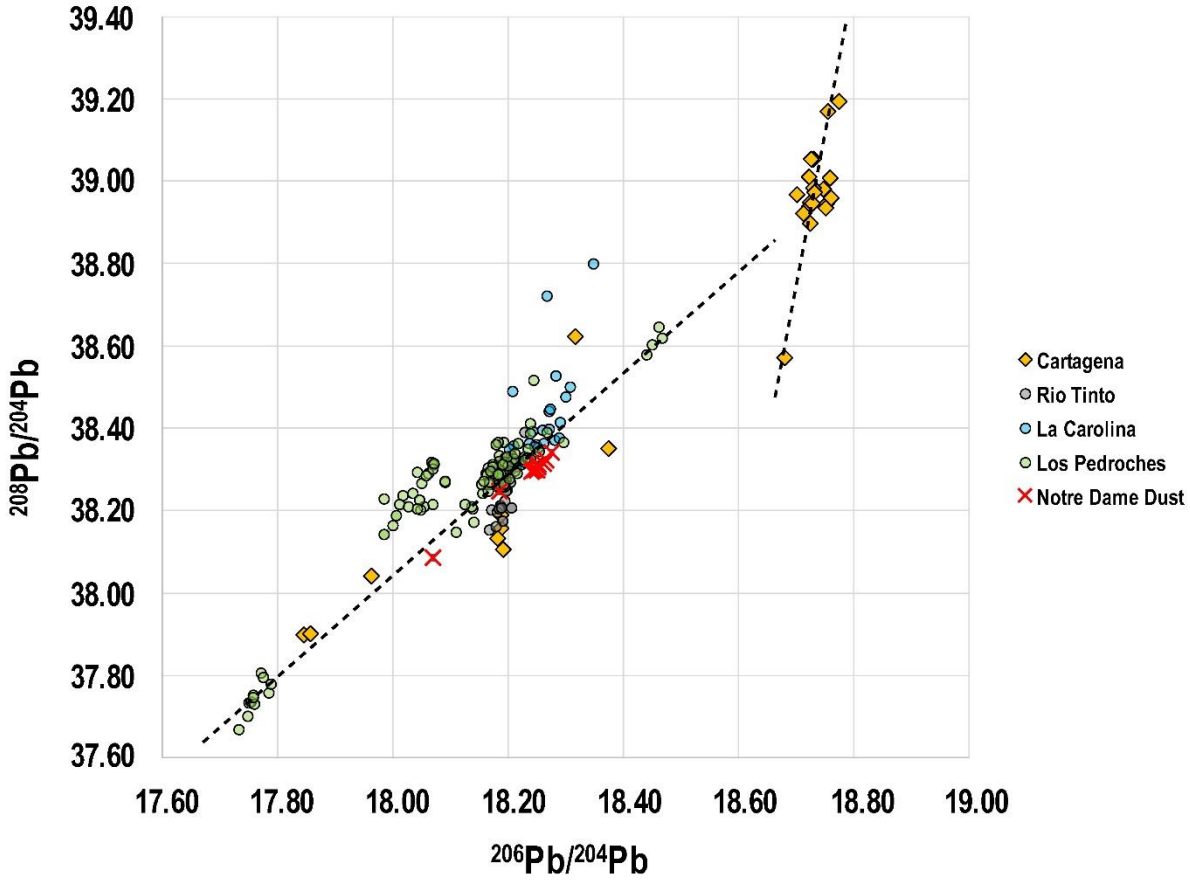
39.40
39.20
39.00
38.80
38.60
38.40
38.20
38.00
37.80
37.60
208Pb/204Pb
17.60
17.80
18.00
18.20
18.40
18.60
18.80
19.00
206Pb/204Pb
Cartagena
Rio Tinto
La Carolina
Los Pedroches
Notre Dame Dust

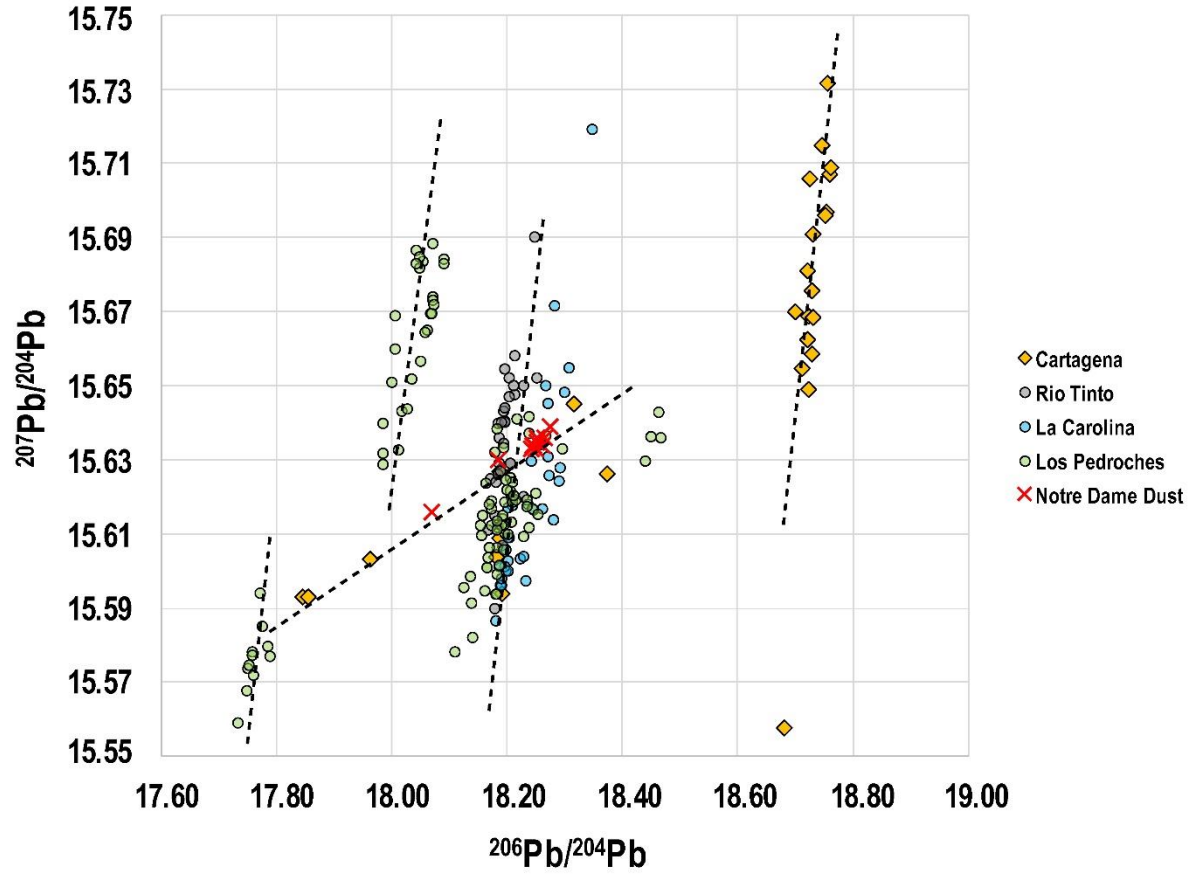
15.75
15.73
15.71
15.69
15.67
15.65
15.63
15.61
15.59
15.57
15.55
207Pb/204Pb
17.60
17.80
18.00
18.20
18.40
18.60
18.80
19.00
206Pb/204Pb
Cartagena
Rio Tinto
La Carolina
Los Pedroches
Notre Dame Dust

509

Figure 6 : $^{208}Pb/^{204}Pb$ versus $^{206}Pb/^{204}Pb$ and $^{207}Pb/^{204}Pb$ versus $^{206}Pb/^{204}Pb$ diagrams of ores signatures from Cartagena (Graeser and Friedrich 1970 ; Marcoux et al., 1992 ; Arribas and Tosdal 1994 ; Stos-Gale and Gale 2009 ; Baron et al., 2017), Rio Tinto (Brill and Wampler 1967 ; Brill et al., 1987 ; Marcoux et al., 1992 ; Marcoux 1998 ; Pomiès et al., 1998 ; Stos-Gale and Gale 2009), La Carolina (Hunt-Ortiz 2003 ; Stos-Gale and Gale 2009 ; Santos-Zalduegui et al., 2004), Los Pedroches (Santos-Zalduegui et al., 2004) and Notre Dame fire dust (This study).

6. Conclusions

We developed an appropriate step-by-step strategy to reveal the samples most representative of the fire emission. A careful and systematic evaluation of the bias due to pre- and post-sampling contamination is an essential tool to trace potential Pb pollution in a city such as Paris where the Pb comes from multiple sources (road traffic, industries, waste incinerators, Pb in habitat and the heritage of the “historical Pb”). In addition, we propose a robust protocol for future dust sampling in historical monuments. The objective is to be able to compare the data in the future (between monuments, after restoration works, and in case of another tragedy).

A 3-step methodology was developed: (1) binocular observations of the macroscopic heterogeneities and subsequent fractioning of the sample into more homogeneous fractions, (2) elemental composition determination for a large range of elements, mainly used to evaluate the impact of the sampling substrate, (3) Pb isotope ratio analysis enabling to reveal more subtle heterogeneities. The smoke plume signature is better represented by the dust fraction of the samples collected on wood substrate on the cathedral’s first floor. This methodology is applicable to the study of Pb sources in historical monuments, to characterize them in an historical perspective, or to evaluate the impacts of an accidental event.

The isotopic and elemental fingerprint highlights the distinctive characteristics of the NDdP fire signature, inherited from the long and rich history of the cathedral. Thus, we propose an uncommon geochemical fingerprint of NDdP fire fallout, characterized by ratios

based on Pb substantially different from classic urban ratios. Most importantly, the NDdP fire Pb isotope ratio signature is finely characterized with median values of 206Pb/207Pb ratio: 1.16738±0.00057 and 208Pb/206Pb ratio: 2.09875±0.00049.

In a further step, this signature will be used to trace this major event in the Parisian environment. The fire Pb signature is distinct from today's urban Pb signature, which is imprinted by the leaded gasoline used during the second half of the 20th century. This leaves some space to distinguish the NDdP fire Pb inputs from the urban contamination preexisting the 2019 fire in environmental reservoirs (soils, river sediments, atmospheric particles).

Finally, we showed that the Pb contained in the NDdP fire dusts seems to have originated from Cartagena mining district, more precisely from the least radiogenic group of Cartagena ores.

Acknowledgments

The authors thank the CNRS, more specifically the "Mission pour les Initiatives Transverses et Interdisciplinaires (MITI)" and the Research Group ReMArch « Remploi et Recyclage des Matériaux de l'Architecture », CNRS (GDR 2063) for their financial support. This work is part of the research conducted by the Group Metals of the Chantier Scientifique de Notre-Dame (CNRS/Ministère de la Culture). The authors thank all its members for the scientific discussions.

Supporting information:

Word file:

Table S1 Location and description of samples collected in NDdP

Table S3. Elemental composition (mg.kg^{-1}) and lead isotope ratio for the certified reference materials

Fig. S1. Lead isotopic compositions determined at LSCE and CRPG laboratories.

Fig. S2. Lead isotopic compositions of heterogeneous samples from this study.

Fig. S3. Bivariate concentration plots of selected element versus Pb concentrations for heterogeneous samples (*i.e.,* presenting a 'dust only' fraction and a 'fiber and dust' fraction')

Excel Files:

Table S2. Selected isotopes and analysis modes of elements.

Table S4. Elemental and lead isotope ratios of NDdP samples.

Table S5. Lead isotope ratios of the Sainte-Chapelle and Chartres cathedral lead samples.

Table S6. Composition of the "only dust" and "fiber and dust" fractions for four NDdP samples.

Table S7. Lead isotope ratios of the dust samples representative of NDdP fire (SARM)

References

Amodio, M., Catino, S., Dambruoso, P. R., De Gennaro, G., Di Gilio, A., Giungato, P., Laiola, E., Marzocca, A., Mazzone, A., Sardaro, A., & Tutino, M. (2014). Atmospheric deposition: sampling procedures, analytical methods, and main recent findings from the scientific literature. Advances in Meteorology, 2014. https://doi.org/10.1155/2014/161730.

Arribas, A., & Tosdal, R. M. (1994). Isotopic composition of Pb in ore deposits of the Betic Cordillera, Spain; origin and relationship to other European deposits. Economic Geology, 89(5), 1074-1093. https://doi.org/10.2113/gsecongeo.89.5.1074.

Aubert, M. (1920). Notre-Dame de Paris: sa place dans l'histoire de l'architecture du XIIe au XIVe siècle. H. Laurens.

Ayrault, S., Roy-Barman, M., Le Cloarec, M. F., Priadi, C. R., Bonté, P., and Göpel, C. (2012). Lead contamination of the Seine River, France: geochemical implications of a historical perspective. Chemosphere, 87(8), 902-910. https://doi.org/10.1007/s11356-013-2240-6.

Ayrault, S., Le Pape, P., Evrard, O., Priadi, C. R., Quantin, C., Bonté, P., & Roy-Barman, M. (2014). Remanence of lead pollution in an urban river system: a multi-scale temporal and spatial study in the Seine River basin, France. Environmental Science and Pollution Research, 21(6), 4134-4148. https://doi.org/10.1007/s11356-013-2240-6.

Baron, S., Carignan, J., Laurent, S., & Ploquin, A. (2006). Medieval lead making on Mont-Lozère Massif (Cévennes-France): tracing ore sources using Pb isotopes. Applied geochemistry, 21(2), 241-252. https://doi.org/10.1016/j.apgeochem.2005.09.005.

Baron, S., Rico, Ch., et Antolinos Marín, J. A. (2017) : "Le complexe d'ateliers du Cabezo del Pino (Sierra Minera de Cartagena-La Unión, Murcia) et l'organisation de l'activité minière à Carthago Noua à la fin de la République romaine. Apports croisés de l'archéologie et de la géochimie", Archivo Español de Arqueología, 90, 147-169.

Bode, M., Hauptmann, A., & Mezger, K. (2009). Tracing Roman lead sources using lead isotope analyses in conjunction with archaeological and epigraphic evidence—a case study from Augustan/Tiberian Germania. *Archaeological and anthropological* sciences, 1(3), 177-194. https://doi.org/10.1007/s12520-009-0017-0.

Brill, R.H. and Wampler, J. M. (1967). Isotope studies of ancient lead. American Journal of Archaeology 71, 63-77.

Brill, R.H., Barnes, I.L., Tong, S.C., Joel, E.C., Murtaugh, M.J., 1987. Laboratory studies of some European artifacts excavated on San Salvador Island, in: Gerace, D.. (Ed.), Columbus and His World: Proceedings of the First San Salvador Conference. San Salvador, Bahamian Field Station, pp. 247–292

Charlesworth, S., De Miguel, E., & Ordóñez, A. (2011). A review of the distribution of particulate trace elements in urban terrestrial environments and its application to considerations of risk. *Environmental geochemistry and health*, *33*(2), 103-123.

Cheng, H., & Hu, Y. (2010). Lead (Pb) isotopic fingerprinting and its applications in lead pollution studies in China: a review. Environmental pollution, 158(5), 1134-1146. https://doi.org/10.1016/j.envpol.2009.12.028.

Cohen, M. (2008). An Indulgence for the Visitor: The Public at the Sainte-Chapelle of Paris. Speculum, 83(4), 840-883. https://doi.org/10.1017/S003871340001705X.

Comite, V., Pozo-Antonio, J. S., Cardell, C., Rivas, T., Randazzo, L., La Russa, M. F., & Fermo, P. (2019, December). Metals distributions within black crusts sampled on the facade of an historical monument: the case study of the Cathedral of Monza (Milan, Italy). In IMEKO TC4 International Conference on Metrology for Archaeology and Cultural Heritage, MetroArchaeo: 4 through 6 December (pp. 73-78). International Measurement Federation Secretariat (IMEKO).

Delile, H., Keenan-Jones, D., Blichert-Toft, J., Goiran, J. P., Arnaud-Godet, F., Romano, P., & Albarède, F. (2016). A lead isotope perspective on urban development in ancient Naples. Proceedings of the National Academy of Sciences, 113(22), 6148-6153. https://doi.org/10.1073/pnas.1600893113.

Delile, H., Keenan-Jones, D., Blichert-Toft, J., Goiran, J. P., Arnaud-Godet, F., & Albarède, F. (2017). Rome's urban history inferred from Pb-contaminated waters trapped in its ancient harbor basins. Proceedings of the National Academy of Sciences, 114(38), 10059-10064. https://doi.org/10.1073/pnas.1706334114.

Elbaz-Poulichet, F., Holliger, P., Martin, J. M., & Petit, D. (1986). Stable lead isotopes ratios in major French rivers and estuaries. Science of the Total Environment, 54, 61-76. https://doi.org/10.1016/0048-9697(86)90256-1.

Ellam, R. M. (2010). The graphical presentation of lead isotope data for environmental source apportionment. Science of the Total Environment, 408(16), 3490-3492.

Farmer, J. G., Eades, L. J., Atkins, H., & Chamberlain, D. F. (2002). Historical trends in the lead isotopic composition of archival Sphagnum mosses from Scotland (1838− 2000). Environmental science & technology, 36(2), 152-157.

Font, A., de Hoogh, K., Leal-Sanchez, M., Ashworth, D. C., Brown, R. J., Hansell, A. L., & Fuller, G. W. (2015). Using metal ratios to detect emissions from municipal waste incinerators in ambient air pollution data. Atmospheric environment, 113, 177-186. https://doi.org/10.1016/j.atmosenv.2015.05.002.

Gasperi, J., Le Roux, J., Deshayes, S., Ayrault, S., Bordier, L., Boudahmane, L., ... & Gromaire, M. C. (2022). Micropollutants in Urban Runoff from Traffic Areas: Target and Non-Target Screening on Four Contrasted Sites. *Water*, *14*(3), 394.

van Geen, A., Yao, Y., Ellis, T., & Gelman, A. (2020). Fallout of lead over Paris from the 2019 Notre-Dame cathedral fire. *GeoHealth*, *4*(8), e2020GH000279. https://doi.org/10.1029/2020GH000279.

Gillies, J. A., Gertler, A. W., Sagebiel, J. C., & Dippel, N. W. (2001). On-road particulate matter (PM2. 5 and PM10) emissions in the Sepulveda Tunnel, Los Angeles, California. Environmental science & technology, 35(6), 1054-1063. https://doi.org/10.1021/es991320p.

Glorennec, P., Peyr, C., Poupon, J., Oulhote, Y., & Le Bot, B. (2010). Identifying sources of lead exposure for children, with lead concentrations and isotope ratios. Journal of occupational and environmental hygiene, 7(5), 253-260. https://doi.org/10.1080/15459621003648281.

Graeser, S., Friedrich, G., 1970. Zur Frage der Altersstellung und Genese der Blei-Zink-Vorkommen der Sierra de Cartagena in Spanien. Miner. Depos. 5, 365–374.

Hunt-Ortiz, M.A., 2003. Prehistoric Mining and Metallurgy in South West Iberian Peninsula. Britisch Archaeologicla Reports. S1188. 9781841715544 (paperback) , 9781407325958 (ebook)

Harju, L., Lill, J. O., Saarela, K. E., Heselius, S. J., Hernberg, F. J., & Lindroos, A. (1996). Study of seasonal variations of trace-element concentrations within tree rings by thick-target PIXE analyses. Nuclear Instruments and Methods in Physics Research Section B: Beam Interactions with Materials and Atoms, 109, 536-541.

Jørgensen, Søren Storgaard, and Marta Willems. 1987. "The fate of lead in soils: Lead originating from roofs of ancient churches." *Ambio*:16-19.

Laidlaw, M. A., and Taylor, M. P. (2011). Potential for childhood lead poisoning in the inner cities of Australia due to exposure to lead in soil dust. Environmental Pollution, 159(1), 1-9. https://doi.org/10.1016/j.envpol.2010.08.020.

Laidlaw, M. A., Filippelli, G. M., Brown, S., Paz-Ferreiro, J., Reichman, S. M., Netherway, P., Truskewycz, A., Ball, A. S., and Mielke, H. W. (2017). Case studies and evidence-based approaches to addressing urban soil lead contamination. Applied Geochemistry, 83, 14-30. https://doi.org/10.1016/j.apgeochem.2017.02.015.

Landrigan, P.J., Fuller, R., Acosta, N. J. R., Adeyi, O., Arnold, R., Basu, N., Balde, A.B., Bertollini, R., Bose-O'Reilly, S., Boufford, J.I., Breysse, P.N., Chiles, T., Mahidol, C., Coll-Seck, A.M., Cropper, M.L., Fobil, J., Fuster, V., Greenstone, M., Haines, A., Hanrahan, D.,Hunter, D., Khare, M., Krupnick, A., Lanphear, B., Lohani, B., Martin, K., Mathiasen, K. V., McTeer, M. A., Murray, C. J. L., Ndahimananjara, J. D., Perera, F., Potocnik, J., Preker, A. S., Ramesh, J., Rockstrom, J., Salinas, C., Samson, L. D., Sandilya, K., Sly, P. D., Smith, K. R., Steiner, A., Stewart, R. B., Suk, W. A., van Schayck, O. C. P., Yadama, G. N., Yumkella, K. ,Zhong, M. 2017. The Lancet Commission on pollution and health. Lancet 2018, 391:464–512. http://dx.doi.org/10.1016/S0140-6736(17)32345-0.

Le Gall, M., Ayrault, S., Evrard, O., Laceby, J. P., Gateuille, D., Lefèvre, I., Mouchel, J. M., and Meybeck, M. (2018). Investigating the metal contamination of sediment transported by the 2016 Seine River flood (Paris, France). Environmental Pollution, 240, 125-139. https://doi.org/10.1016/j.envpol.2018.04.082

Lestel, Laurence. 2012. "Non-ferrous metals (Pb, Cu, Zn) needs and city development: the Paris example (1815–2009)." *Regional Environmental Change* 12 (2):311-323.

L'Héritier, M., Arles, A., Disser, A., & Gratuze, B. (2016). Lead it be! Identifying the construction phases of gothic cathedrals using lead analysis by LA-ICP-MS. Journal of Archaeological Science: Reports, 6, 252-265. https://doi.org/10.1016/j.jasrep.2016.02.017.

Lin, Y. C., Tsai, C. J., Wu, Y. C., Zhang, R., Chi, K. H., Huang, Y. T., Lin, S. H., & Hsu, S. C. (2015). Characteristics of trace metals in traffic-derived particles in Hsuehshan Tunnel, Taiwan: size distribution, potential source, and fingerprinting metal ratio. Atmospheric Chemistry and Physics, 15(8), 4117-4130. https://doi.org/10.5194/acp-15-4117-2015.

Manhes, G., Allègre, C. J., Dupré, B., & Hamelin, B. (1980). Lead isotope study of basic-ultrabasic layered complexes: Speculations about the age of the earth and primitive mantle characteristics. Earth and Planetary Science Letters, 47(3), 370-382.

Marcoux, E., Leistel, J. M., Sobol, F., Milesi, J. P., & Lescuyer, J. L. (1992). Signature isotopique du plomb des amas sulfurés de la province de Huelva, Espagne. Conséquences métallogéniques et géodynamiques. Comptes rendus de l'Académie des sciences. Série 2, Mécanique, Physique, Chimie, Sciences de l'univers, Sciences de la Terre, 314(13), 1469-1476.

Marcoux, E., Leistel, J.M., Sobol, J., Milesi, J.P., Lescuyer, J.L., Leca, X., 1992. Signature isotopique du plomb des amas sulfurés de la province de Huelva, Espagne. Conséquences métallogéniques et géodynamiques. C.R. Acad. Sci. Paris 314, 1469–1476.

Marcoux, E., 1998. Lead isotope systematics of the giant massive sulphide deposits in the Iberian Pyrite Belt. Mineralium Deposita, 33, 45–58.

Marx, S. K., Rashid, S., & Stromsoe, N. (2016). Global-scale patterns in anthropogenic Pb contamination reconstructed from natural archives. *Environmental Pollution*, *213*, 283-298. https://doi.org/10.1016/j.envpol.2016.02.006.

Monna, F., Lancelot, J., Croudace, I. W., Cundy, A. B., & Lewis, J. T. (1997). Pb isotopic composition of airborne particulate material from France and the southern United Kingdom: implications for Pb pollution sources in urban areas. Environmental Science & Technology, 31(8), 2277-2286. https://doi.org/10.1021/es960870.

Pio, C., Mirante, F., Oliveira, C., Matos, M., Caseiro, A., Oliveira, C., Querol, X., Alves, C., Martins, N., Cerqueira, M., Camões, F., Silva, H., & Plana, F. (2013). Size-segregated chemical composition of aerosol emissions in an urban road tunnel in Portugal. Atmospheric Environment, 71, 15-25. https://doi.org/10.1016/j.atmosenv.2013.01.037.

Pomiès, C., Cocherie, A., Guerrot, C., Marcoux, E., & Lancelot, J. (1998). Assessment of the precision and accuracy of lead-isotope ratios measured by TIMS for geochemical applications: example of massive sulphide deposits (Rio Tinto, Spain). Chemical Geology, 144(1-2), 137-149. https://doi.org/10.1016/S0009-2541(97)00127-7.

Pons-Branchu, E., Ayrault, S., Roy-Barman, M., Bordier, L., Borst, W., Branchu, P., Douville, E., & Dumont, E. (2015). Three centuries of heavy metal pollution in Paris (France) recorded by urban speleothems. Science of the total environment, 518, 86-96. https://doi.org/10.1016/j.scitotenv.2015.02.071.

Resongles, E., Dietze, V., Green, D. C., Harrison, R. M., Ochoa-Gonzalez, R., Tremper, A. H., & Weiss, D. J. (2021). Strong evidence for the continued contribution of lead deposited during the 20th century to the atmospheric environment in London of today. Proceedings of the National Academy of Sciences, 118(26). https://doi.org/10.1073/pnas.2102791118.

Rosca, C., Tomlinson, E. L., Geibert, W., McKenna, C. A., Babechuk, M. G., & Kamber, B. S. (2018). Trace element and Pb isotope fingerprinting of atmospheric pollution sources: A case study from the east coast of Ireland. Applied Geochemistry, 96, 302-326. https://doi.org/10.1016/j.apgeochem.2018.07.003.

Saarela, K. E., Harju, L., Rajander, J., Lill, J. O., Heselius, S. J., Lindroos, A., & Mattsson, K. (2005). Elemental analyses of pine bark and wood in an environmental study. Science of the Total Environment, 343(1-3), 231-241.

Santos Zalduegui, J. F., García de Madinabeitia, S., Gil Ibarguchi, J. I., & Palero, F. (2004). A lead isotope database: the Los Pedroches–Alcudia area (Spain); implications for archaeometallurgical connections across southwestern and southeastern Iberia. Archaeometry, 46(4), 625-634. https://doi.org/10.1111/j.1475-4754.2004.00178.x.

Sawidis, T., Breuste, J., Mitrovic, M., Pavlovic, P., & Tsigaridas, K. (2011). Trees as bioindicator of heavy metal pollution in three European cities. Environmental pollution, 159(12), 3560-3570. https://doi.org/10.1016/j.envpol.2011.08.008.

Shelby, L. R. (1981). Review of the book “The contractors of Chartres” by John James, 1979. Speculum, 56(2), 395-398.

Shotyk, William, Jiancheng Zheng, Michael Krachler, Christian Zdanowicz, Roy Koerner, and David Fisher. 2005. "Predominance of industrial Pb in recent snow (1994–2004) and ice (1842–1996) from Devon Island, Arctic Canada." *Geophysical Research Letters* 32 (21).

Smith, K. E., Weis, D., Amini, M., Shiel, A. E., Lai, V. W. M., & Gordon, K. (2019). Honey as a biomonitor for a changing world. Nature Sustainability, 2(3), 223-232. https://doi.org/10.1038/s41893-019-0243-0.

Smith, K. E., Weis, D., Chauvel, C., & Moulin, S. (2020). Honey maps the pb fallout from the 2019 fire at notre-dame cathedral, paris: A geochemical perspective. Environmental Science & Technology Letters, 7(10), 753-759. https://doi.org/10.1021/acs.estlett.0c00485.

Stos-Gale, Z. A. and Gale, N. H. (2009). Metal provenancing using isotopes and the Oxford archaeological lead isotope database. Archaeological and anthropological Sciences, 1, 195-213.

Syvilay, D., Texier, A., Arles, A., Gratuze, B., Wilkie-Chancellier, N., Martinez, L., Serfaty, S., & Detalle, V. (2015). Trace element quantification of lead based roof sheets of historical monuments by laser induced breakdown spectroscopy. Spectrochimica Acta Part B: Atomic Spectroscopy, 103, 34-42. https://doi.org/10.1016/j.sab.2014.10.013.

Thirlwall, M. F. (2002). Multicollector ICP-MS analysis of Pb isotopes using a 207Pb-204Pb double spike demonstrates up to 400 ppm/amu systematic errors in Tl-normalization. Chemical Geology, 184(3-4), 255-279.

Tognet, F., & Truchot, B. (2019). Modélisation de la Dispersion des Particules de Plomb du Panache de L’incendie de Notre Dame. Ineris-200480-879062-v2. 0.

Vallée, A., Sorbets, E., Lelong, H., Langrand, J., & Blacher, J. (2021). The lead story of the fire at the Notre-Dame cathedral of Paris. Environmental Pollution, 269, 116140. https://doi.org/10.1016/j.envpol.2020.116140.

Vanderstraeten, A., Bonneville, S., Gili, S., De Jong, J., Debouge, W., Claeys, P., & Mattielli, N. (2020). First Multi-Isotopic (Pb-Nd-Sr-Zn-Cu-Fe) Characterisation of Dust Reference Materials (ATD and BCR-723): A Multi-Column Chromatographic Method Optimised to Trace Mineral and Anthropogenic Dust Sources. Geostandards and Geoanalytical Research, 44(2), 307-329.

Véron, A., Flament, P., Bertho, M. L., Alleman, L., Flegal, R., & Hamelin, B. (1999). Isotopic evidence of pollutant lead sources in Northwestern France. Atmospheric Environment, 33(20), 3377-3388. https://doi.org/10.1016/S1352-2310(98)00376-8.

Watmough, S. A., & Hutchinson, T. C. (1996). Analysis of tree rings using inductively coupled plasma mass spectrometry to record fluctuations in a metal pollution episode. Environmental Pollution, 93(1), 93-102. https://doi.org/10.1016/0269-7491(95)00107-7.

Widory, D., Roy, S., Le Moullec, Y., Goupil, G., Cocherie, A., & Guerrot, C. (2004). The origin of atmospheric particles in Paris: a view through carbon and lead isotopes. Atmospheric Environment, 38(7), 953-961. https://doi.org/10.1016/j.atmosenv.2003.11.001.

Wyttenbach, A., & Schubiger, P. A. (1973). Trace element content of Roman lead by neutron activation analysis. Archaeometry, 15(2), 199-207. https://doi.org/10.1111/j.1475-4754.1973.tb00090.x.

Yu, K. F., Kamber, B. S., Lawrence, M. G., Greig, A., & Zhao, J. X. (2007). High-precision analysis on annual variations of heavy metals, lead isotopes and rare earth elements in mangrove tree rings by inductively coupled plasma mass spectrometry. Nuclear Instruments and Methods in Physics Research Section B: Beam Interactions with Materials and Atoms, 255(2), 399-408. https://doi.org/10.1016/j.nimb.2006.11.127.

White, W. M., Albarède, F., & Télouk, P. (2000). High-precision analysis of Pb isotope ratios by multi-collector ICP-MS. Chemical Geology, 167(3-4), 257-270.